applied optics

Quantifying polarization changes induced by rotating Dove prisms and K-mirrors

Suman Karan,[1,2,†] Ruchi,[1,3,†] Pranay Mohta,[1] and Anand K. Jha[1,*]

[1]Department of Physics, Indian Institute of Technology Kanpur, Kanpur, Uttar Pradesh 208016, India
[2]e-mail: karans@iitk.ac.in
[3]e-mail: ruchirajput19@gmail.com
*Corresponding author: akjha@iitk.ac.in

Received 9 August 2022; revised 4 September 2022; accepted 5 September 2022; posted 6 September 2022; published 22 September 2022

Dove prisms and K-mirrors are devices extensively used for rotating the wavefront of an optical field. These devices have several applications, including the measurement of orbital angular momentum, microscopy, beam steering, and pattern recognition. However, the wavefront rotation achieved through these devices is always accompanied by polarization changes in the incident field, which is an undesirable feature in many of these applications. Although the polarization changes induced by a Dove prism have been explored to quite some extent, no such study is available for a K-mirror. In this paper, we theoretically and experimentally investigate polarization changes induced in the transmitted field by a rotating K-mirror. For quantifying such polarization changes, we define a quantity, mean polarization change D, which ranges from 0 to π. We find that K-mirrors can reduce D to about 0.03π for any incident state of polarization; however, reducing D to the same extent with a Dove prism is practically unviable. Therefore, K-mirrors are better alternatives to Dove prisms in applications in which the polarization changes accompanying wavefront rotation need to be minimum.

https://doi.org/10.1364/AO.472543

Rotation of an optical wavefront by an arbitrary angle is desirable in several applications. Various kinds of devices, such as Dove prisms [1], Pechan prisms [2], K-shape prisms [3], Porro prisms [4], and rotators based on mirror reflections [5–8] are used to achieve the rotation of an incident optical wavefront. Among these, Dove prisms are widely used due to their applications in interferometry [9–11], microscopy [12], beam steering [13], optical astronomy [14], pattern recognition [15], and sensing based on surface plasmon resonance [16]. In recent years, Dove prisms have also been used in optical profilers [17], in optical parametric oscillators [18], and for measuring orbital angular momentum (OAM) of a single photon [3,4,19–22].

Despite having a plethora of applications, a Dove prism has major alignment issues in experiments in which it needs to be rotated. A Dove prism is a single-piece device; thus, one cannot adjust the angles between different reflecting or refracting surfaces. This invariably causes finite lateral and angular shifts of the field transmitting through it. It is a major concern in applications where rotation of an incident field with respect to a fixed center is desired. Even in the case of interferometric measurements, a shift of the field leads to additional temporal fringes and thus affects the visibility. In order to overcome these challenges, a K-mirror is often employed to rotate an optical wavefront [5–7]. A K-mirror consists of three separate mirrors with independent controls that can be used to minimize the lateral and angular shifts to a great extent [6]. Therefore, although Dove prisms are convenient in several applications, K-mirrors are a better alternative where continuous rotation of a wavefront is required. Recently, K-mirrors have been used in the measurement of the OAM spectrum of partially coherent fields [7] and the spiral spectrum of photon pairs generated by spontaneous parametric down-conversion [5].

The working of a Dove prism or a K-mirror is highly dependent on the polarization of the incident field [3,5,7,20]. As a result, the wavefront rotation achieved through these devices is always accompanied by polarization changes in the transmitted field. This is an undesirable feature in many applications. Since a K-mirror involves three reflections while a Dove prism involves two refractions and one total internal reflection, the wavefront rotation through these two devices can cause different polarization changes in the transmitted field. Although the polarization changes induced by a Dove prism have been explored to quite some extent [1,2,23], no such study is available for a K-mirror. In this paper, we theoretically and experimentally investigate polarization changes induced in the transmitted field by a rotating K-mirror.

Consider a Dove prism with base angle α and a K-mirror with base angle β as shown in Fig. 1(a) and 1(b), respectively. As can be inferred from Fig. 1, α ranges from 0° to 90°, while β ranges

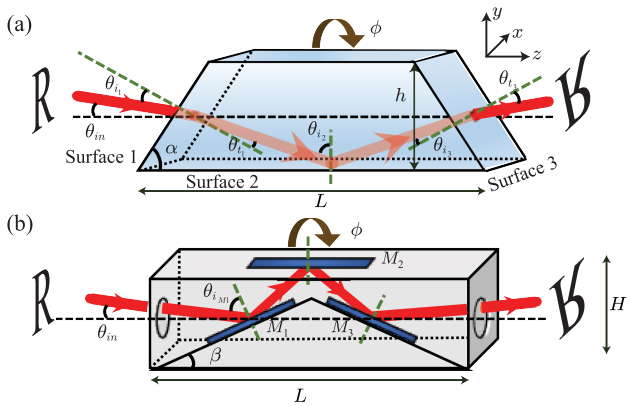

Fig. 1. (a) Schematic of the field transmission through a Dove prism having base angle α. (b) Schematic of the field transmission through a K-mirror having base angle β.

from 0° to 45°. Here we work out a quantifier of polarization changes induced in the incident field for the rotation of the devices from $\phi = 0$ to $\phi = \pi$. We take the electric field incident onto the Dove prism or the K-mirror as $\boldsymbol{E}^{\text{in}} = E_x^{\text{in}}\hat{\boldsymbol{x}} + E_y^{\text{in}}\hat{\boldsymbol{y}}$, where $E_x^{\text{in}} = \cos\psi_{\text{in}}$ and $E_y^{\text{in}} = \sin\psi_{\text{in}}e^{i\delta_{\text{in}}}$ are x- and y-polarized components of the electric field (see Fig. 1.) The state of polarization (SOP) of the incident field $\boldsymbol{E}^{\text{in}}$ is uniquely represented by the Stokes vector $\mathbf{S}^{\text{in}}$, given as $\mathbf{S}^{\text{in}} = [S_0^{\text{in}} \quad S_1^{\text{in}} \quad S_2^{\text{in}} \quad S_3^{\text{in}}]^T$, where the Stokes parameters are given by $S_0^{\text{in}} = |E_x^{\text{in}}|^2 + |E_y^{\text{in}}|^2$, $S_1^{\text{in}} = |E_x^{\text{in}}|^2 - |E_y^{\text{in}}|^2$, $S_2^{\text{in}} = 2\text{Re}[E_x^{\text{in}*}E_y^{\text{in}}]$, and $S_3^{\text{in}} = 2\text{Im}[E_x^{\text{in}*}E_y^{\text{in}}]$ [24]. The normalized Stokes parameters $\bar{\boldsymbol{S}}^{\text{in}}$ are represented by a point on the surface of the Poincaré sphere of radius equal to $\bar{S}_0^{\text{in}} = 1$ as shown in Fig. 2, where $\bar{S}_0^{\text{in}} = S_0^{\text{in}}/S_0^{\text{in}}$, $\bar{S}_1^{\text{in}} = S_1^{\text{in}}/S_0^{\text{in}}$, $\bar{S}_2^{\text{in}} = S_2^{\text{in}}/S_0^{\text{in}}$, and $\bar{S}_3^{\text{in}} = S_3^{\text{in}}/S_0^{\text{in}}$. We represent the incident polarization state by the black dot P_{in} on the Poincaré sphere. When a Dove prism or a K-mirror is rotated from 0° to 180°, the transmitted state of polarization forms a closed loop on the Poincaré sphere, as shown by the blue curve in Fig. 2. For illustrating the sense of rotation, we show P_1, P_2, P_3, P_4 on the Poincaré sphere, which are the states of polarization of the transmitted field at $\phi = 20°, 60°, 100°$ and $140°$, respectively.

The field transmitted through a device at the rotation angle ϕ can be written as $\boldsymbol{E}^{\text{out}} = T_j\boldsymbol{E}^{\text{in}}$, where $j = [\text{DP}, \text{KM}]$. T_{DP} and T_{KM} stand for the transfer matrix for transmission corresponding to a Dove prism and a K-mirror, respectively (see Supplement 1, sections 1, 2, and 3 for the detailed calculations of T_{DP} and T_{KM}). Thus, the transmitted field $\boldsymbol{E}^{\text{out}}$ can be shown to be

$$\begin{bmatrix} E_x^{\text{out}} \\ E_y^{\text{out}} \end{bmatrix} = \begin{bmatrix} \left(T_j^s\cos^2\phi + T_j^p\sin^2\phi\right)\cos\psi_{\text{in}} \\ +\left(T_j^s - T_j^p\right)\sin\phi\cos\phi\sin\psi_{\text{in}}e^{i\delta_{\text{in}}} \\ \left(T_j^s - T_j^p\right)\sin\phi\cos\phi\cos\psi_{\text{in}} \\ +\left(T_j^p\cos^2\phi + T_j^s\sin^2\phi\right)\sin\psi_{\text{in}}e^{i\delta_{\text{in}}} \end{bmatrix}. \tag{1}$$

The state of polarization of the transmitted field is represented by the Stokes vector $\mathbf{S}^{\text{out}}$. The Stokes parameters can be calculated in terms of the transmitted field and can be shown to be

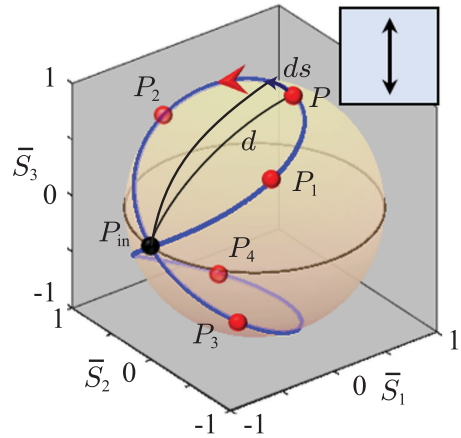

Fig. 2. Poincaré sphere representation of the polarization states of the transmitted field as a function of the rotation angle ϕ. As shown in the inset and by the black dot on the Poincaré sphere, the incident polarization is vertical. The geodesic distance d is the difference between the transmitted state of polarization P and the incident SOP P_{in}. ds depicts the arc length element.

$$\begin{aligned} S_0^{\text{out}} &= |E_x^{\text{out}}|^2 + |E_y^{\text{out}}|^2 \\ &= \frac{1}{4}\Big[2|T_j^s|^2 + |T_j^p|^2 + \cos 2\psi_{\text{in}}\big\{|T_j^p|^2 - 2\big(|T_j^p|^2 \\ &\quad - |T_j^s|^2\big)\cos 2\phi\big\} + 2|T_j^p|^2\sin^2\psi_{\text{in}} \\ &\quad - 2\big(|T_j^p|^2 - |T_j^s|^2\big)\cos\delta_{\text{in}}\sin 2\psi_{\text{in}}\sin 2\phi\Big], \end{aligned} \tag{2}$$

$$\begin{aligned} S_1^{\text{out}} &= |E_x^{\text{out}}|^2 - |E_y^{\text{out}}|^2 \\ &= \frac{1}{4}\Big[2\left(|T_j^s|^2 - |T_j^p|^2\right)\cos 2\phi + \big\{|T_j^s|^2 + |T_j^p|^2 \\ &\quad + \left(|T_j^s|^2 + |T_j^p|^2\right)\cos 4\phi + 4\text{Re}\left[T_j^s T_j^{p*}\right]\sin^2 2\phi\big\}\cos 2\psi_{\text{in}} \\ &\quad + \big\{-4\text{Im}\left[T_j^s T_j^{p*}\right]\sin\delta_{\text{in}}\sin 2\phi + \big(|T_j^s|^2 + |T_j^p|^2 \\ &\quad - 2\text{Re}\left[T_j^s T_j^{p*}\right]\big)\cos\delta_{\text{in}}\sin 4\phi\big\}\sin 2\psi_{\text{in}}\Big], \end{aligned} \tag{3}$$

$$\begin{aligned} S_2^{\text{out}} &= 2\text{Re}\left[E_x^{\text{out}*}E_y^{\text{out}}\right] \\ &= \frac{1}{4}\Big[\big\{|T_j^s|^2 + |T_j^p|^2 + 2\text{Re}\left[T_j^s T_j^{p*}\right] - \big(|T_j^s|^2 + |T_j^p|^2 \\ &\quad - 2\text{Re}\left[T_j^s T_j^{p*}\right]\big)\cos 4\phi\big\}\cos\delta_{\text{in}}\sin 2\psi_{\text{in}} \\ &\quad + 4\text{Im}\left[T_j^s T_j^{p*}\right]\cos 2\phi\sin\delta_{\text{in}}\sin 2\psi_{in} + 2\left(|T_j^s|^2 - |T_j^p|^2\right)\sin 2\phi \\ &\quad + \big(|T_j^s|^2 + |T_j^p|^2 - 2\text{Re}\left[T_j^s T_j^{p*}\right]\big)\cos 2\psi_{\text{in}}\sin 4\phi\Big], \end{aligned} \tag{4}$$

$$\begin{aligned} S_3^{\text{out}} &= 2\text{Im}\left[E_x^{\text{out}*}E_y^{\text{out}}\right] \\ &= \left(\text{Im}\left[T_j^s T_j^{p*}\right]\cos\delta_{\text{in}}\cos 2\phi - \text{Re}\left[T_j^s T_j^{p*}\right]\sin\delta_{\text{in}}\right)\sin 2\psi_{\text{in}} \\ &\quad - \text{Im}\left[T_j^s T_j^{p*}\right]\cos 2\psi_{\text{in}}\sin 2\phi, \end{aligned} \tag{5}$$

where Re[$\cdots$] and Im[$\cdots$] represent the real and imaginary parts, respectively. Next, we calculate the normalized Stokes parameters as $\bar{S}_0^{\text{out}} = S_0^{\text{out}}/S_0^{\text{out}}$, $\bar{S}_1^{\text{out}} = S_1^{\text{out}}/S_0^{\text{out}}$, $\bar{S}_2^{\text{out}} = S_2^{\text{out}}/S_0^{\text{out}}$, and $\bar{S}_3^{\text{out}} = S_3^{\text{out}}/S_0^{\text{out}}$. We plot these normalized Stokes parameters on the Poincaré sphere as a function of ϕ.

In order to quantify the polarization changes, we take the geodesic distance d as an estimate of the difference between a transmitted state of polarization P and the incident state of polarization P_{in} (see Fig. 2.) The geodesic distance d is given by

$$d = \cos^{-1}\left[\bar{S}_1^{\text{out}}\bar{S}_1^{\text{in}} + \bar{S}_2^{\text{out}}\bar{S}_2^{\text{in}} + \bar{S}_3^{\text{out}}\bar{S}_3^{\text{in}}\right]. \tag{6}$$

Next, for estimating the overall polarization change induced by a device when it is rotated from $\phi = 0$ to $\phi = \pi$, we define the mean polarization change D as the average geodesic distance d over a closed loop on the Poincaré sphere. We thus write D as

$$D = \frac{\int d\,\mathrm{d}s}{\int \mathrm{d}s} = \frac{\int_{\phi=0}^{\pi} \cos^{-1}\left[\sum_{i=1}^{3} \bar{S}_i^{\text{out}}\bar{S}_i^{\text{in}}\right]\sqrt{\sum_{i=1}^{3}\left(\frac{d\bar{S}_i^{\text{out}}}{d\phi}\right)^2}\,\mathrm{d}\phi}{\int_{\phi=0}^{\pi}\sqrt{\sum_{i=1}^{3}\left(\frac{d\bar{S}_i^{\text{out}}}{d\phi}\right)^2}\,\mathrm{d}\phi}, \tag{7}$$

where $ds = \sqrt{\sum_{i=1}^{3}\left(\frac{d\bar{S}_i^{\text{out}}}{d\phi}\right)^2}\,d\phi$ is the infinitesimal arc length element of the closed loop (see Fig. 2), and where

$$\begin{aligned}\sum_{i=1}^{3}\left(\frac{d\bar{S}_i^{\text{out}}}{d\phi}\right)^2 = \Big[&-4\left(|T_j^{\text{p}}|^2 - |T_j^{\text{s}}|^2\right)^2(\cos\delta_{\text{in}}\cos 2\phi\sin 2\psi_{\text{in}} - \cos 2\psi_{\text{in}}\sin 2\phi)^2 - 16\left(\text{Re}\left[T_j^{\text{s}}T_j^{\text{p}*}\right]^2 - |T_j^{\text{p}}|^2|T_j^{\text{s}}|^2\right)\\
&\times(\cos 2\psi_{\text{in}}\cos 2\phi + \cos\delta_{\text{in}}\sin 2\psi_{\text{in}}\sin 2\phi)^2 + 4\Big[\Big\{\left(|T_j^{\text{s}}|^2 + |T_j^{\text{p}}|^2 - 2\text{Re}\left[T_j^{\text{s}}T_j^{\text{p}*}\right]\right)\cos\delta_{\text{in}}\cos 4\phi\\
&- 2\text{Im}\left[T_j^{\text{s}}T_j^{\text{p}*}\right]\cos 2\phi\sin\delta_{\text{in}}\Big\}\sin 2\psi_{\text{in}} + (|T_j^{\text{p}}|^2 - |T_j^{\text{s}}|^2)\sin 2\phi + \left(2\text{Re}\left[T_j^{\text{s}}T_j^{\text{p}*}\right] - |T_j^{\text{p}}|^2 - |T_j^{\text{s}}|^2\right)\cos 2\psi_{\text{in}}\sin 4\phi\Big]^2\\
&+\Big[\left(|T_j^{\text{s}}|^2 + |T_j^{\text{p}}|^2 - 2\text{Re}\left[T_j^{\text{s}}T_j^{\text{p}*}\right]\right)\cos(2\psi_{\text{in}} - 4\phi) - 4\text{Im}\left[T_j^{\text{s}}T_j^{\text{p}*}\right]\sin\delta_{\text{in}}\sin 2\psi_{\text{in}}\sin 2\phi\\
&- 2\text{Re}\left[T_j^{\text{s}}T_j^{\text{p}*}\right]\left\{\cos(2\psi_{\text{in}} + 4\phi) + 2\cos\delta_{\text{in}}\sin 2\psi_{\text{in}}\sin 4\phi\right\} + |T_j^{\text{p}}|^2\left\{-2\cos 2\phi + \cos(2\psi_{\text{in}} + 4\phi) + 2\cos\delta_{\text{in}}\sin 2\psi_{\text{in}}\sin 4\phi\right\}\\
&+ |T_j^{\text{s}}|^2\left\{2\cos 2\phi + \cos(2\psi_{\text{in}} + 4\phi) + 2\cos\delta_{\text{in}}\sin 2\psi_{\text{in}}\sin 4\phi\right\}\Big]^2\Big]\\
&/\left[|T_j^{\text{p}}|^2 + |T_j^{\text{s}}|^2 - \left(|T_j^{\text{p}}|^2 - |T_j^{\text{s}}|^2\right)\cos 2\psi_{\text{in}}\cos 2\phi - \left(|T_j^{\text{p}}|^2 - |T_j^{\text{s}}|^2\right)\cos\delta_{\text{in}}\sin 2\psi_{\text{in}}\sin 2\phi\right]^2.\end{aligned} \tag{8}$$

D ranges from 0 to π, with $D = 0$ representing no polarization change, while $D = \pi$ represents the maximum polarization change. When $D = 0$, the state of polarization of the transmitted field is same as that of the incident field, whereas when $D = \pi$ the state of polarization of the transmitted field is a point diametrically opposite to P_{in} on the Poincaré sphere.

We now present our numerical studies of polarization change induced by a K-mirror and compare it with that induced by a Dove prism. For our simulations, we consider commercially available Dove prisms and K-mirrors and take the refractive index $n = 1.5168$ for the Dove prism and the refractive index of the silver coating $n_M = 0.1568 + i3.8060$ for the K-mirror. We take the rotation axis of the Dove prism or the K-mirror to be aligned with the direction of propagation of the incident field and thus take $\theta_{\text{in}} = 0$ (see Fig. 1). This is because, at $\theta_{\text{in}} = 0$, the deviation of the transmitted beam at any rotation angle ϕ is minimum, which is necessary for any experimental setup. Therefore, although θ_{in} affects the transmitted polarization state, in this paper, we present all the results at $\theta_{\text{in}} = 0$. We plot the mean polarization change D as a function of the base angles, α and β. Figures 3(a)–3(c) depict D as a function of base angles α and β for linearly, elliptically, and circularly polarized incident fields, respectively. We find that there is no minimum in D for a Dove prism, whereas for a K-mirror D reaches its minimum at around $\beta = 17.88°$. We note that the minimum value of D for linearly, elliptically, and circularly polarized incident fields are 0.0152π, 0.0296π, and 0.0303π, respectively. These are depicted by red dots in Figs. 3(a)–3(c), and the corresponding transmitted fields are shown by the red closed loops on the Poincaré spheres in Figs. 3(d)–3(f). These are tiny closed loops centered at P_{in}, signifying very small polarization changes in the transmitted field. In order to emphasize this, we compare the polarization changes induced by the commercially available Dove prism and K-mirror with $\alpha = 45°$ and $\beta = 32.5°$, respectively. The D values with $\alpha = 45°$ and $\beta = 32.5°$ for three different incident polarizations are depicted by blue and magenta dots in Figs. 3(a)–3(c). The corresponding transmitted fields are shown by blue and magenta closed loops on the Poincaré spheres in Figs. 3(d)–3(f). From the results shown in Fig. 3, we make several observations. We note that while a K-mirror with $\beta = 17.88°$ induces only about 3% mean polarization change with respect to the incident field, the commercially available Dove prism and K-mirror induce much higher changes. Moreover, for different incident states of polarization, the D values induced by a K-mirror with $\beta = 17.88°$ are almost the same, whereas they have wide variations for commercially available Dove prisms and K-mirrors. We further note that there are several pairs of base angles α and β at which a K-mirror and a Dove prism induce the same D. This means that these two devices are equivalent as far as the mean polarization change is concerned; however, the details of polarization changes in the transmitted fields could be different.

Given that a K-mirror at $\beta = 17.88°$ can reduce the induced polarization changes to a much larger extent than the commercially available Dove prisms and K-mirrors, we explore the practical viability of engineering such a K-mirror. First, we

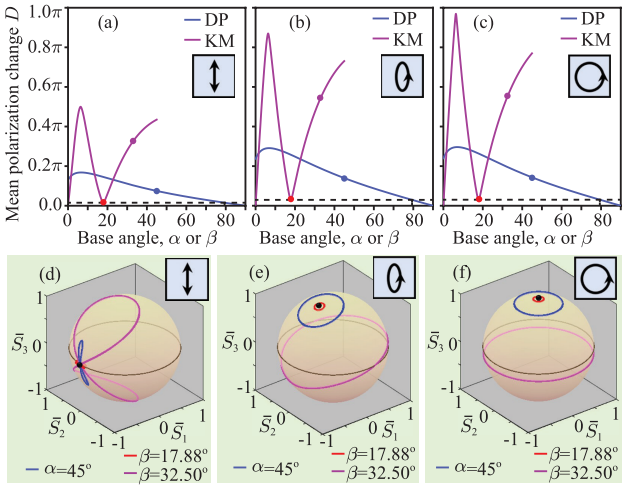

Fig. 3. (a), (b), and (c) Plots of mean polarization change D as a function of the base angle α and β for linearly, elliptically, and circularly polarized incident fields, respectively. The insets show the incident SOP. (d), (e), and (f) Poincaré sphere representations of the transmitted state of polarizations as a function of ϕ. The three closed loops on each Poincaré sphere correspond to the Dove prism base angle $\alpha = 45°$ and the K-mirror base angles $\beta = 17.88°$ and $\beta = 32.5°$.

derive the length L and height H of a K-mirror for a given base angle β and clear aperture h (see Fig. 1). From the geometry of the K-mirror shown in Fig. 1(b), one can show that (see Supplement 1, section 4)

$$L = 2h\cot\beta, \qquad H = \frac{h}{2}\left[1 + \frac{\tan 2\beta}{\tan\beta}\right]. \tag{9}$$

Therefore, for $\beta = 17.88°$ and the commonly used aperture size $h = 2.5$ cm, the length and height of the K-mirror come out to be $L = 15.50$ cm and $H = 4.04$ cm. Thus we see that a K-mirror with $\beta = 17.88°$ is indeed practically viable. From Figs. 3(a)–3(c), we note that, as far as the mean polarization change D is concerned, a Dove prism having $\alpha = 79.41°$ is equivalent to a K-mirror having $\beta = 17.88°$. It is therefore natural to ask whether or not a Dove prism with $\alpha = 79.41°$ is practically viable as well. In order to answer this, we use the L/h ratio derived in Refs. [1,25], which is given by $\frac{L}{h} = \frac{1}{\sin 2\alpha}[1 + \frac{\sqrt{n^2 - \cos^2\alpha} + \sin\alpha}{\sqrt{n^2 - \cos^2\alpha} - \sin\alpha}]$, where L is the length and h is the aperture size of the Dove prism. Thus for the base angle $\alpha = 79.41°$ and clear aperture size $h = 2.5$ cm, the required length of a Dove prism is $L = 39.88$ cm. Therefore, although it is practically viable to reduce the mean polarization change D to about 3% using a K-mirror, it is almost impractical to reduce D to such an extent using a Dove prism. Even if such a Dove prism is possible to produce, it will not be useful for several reasons, including the much increased lateral and angular shifts and the instability of tabletop interferometric setups due to the increased size of the interferometer.

So far, we have only explored K-mirrors with silver coating for reducing the mean polarization change D. We next explore the effects of the other commonly used metal coatings on D. For each metal coating, we evaluate the attributes of the K-mirror that minimizes D. In Table 1, we report the base angle β, the length L, the height H, and the minimum value of D for the three most commonly used coatings, namely aluminum, gold, and silver. We thus find that the silver coating is the best in minimizing the mean polarization change.

We next present our experimental studies of the polarization changes induced in the transmitted field by the commercially available Dove prism ($\alpha = 45°$) and K-mirror ($\beta = 32.5°$). In our experiment, we use Thorlabs Dove prism (PS992M-B) and a Science Edge K-mirror (IRMU-25-A). The experimental setup is shown in Fig. 4. We use a 5 mW vertically polarized Newport He–Ne laser and generate different incident states of polarization using a half-wave plate H and a quarter-wave plate Q_1. The incident field passes through the Dove prism or the K-mirror mounted on a rotating stage whose rotation axis coincides with the incident field's propagation direction such that $\theta_{in} = 0$ (see Fig. 1). We perform polarization tomography on the transmitted field and measure the corresponding Stokes parameters using a polarizer and a quarter-wave plate [24]. Figures 5(d)–5(f) represent the experimentally observed transmitted SOP on the Poincaré sphere as a function of the rotation angle ϕ of the Dove prism for linearly, elliptically, and circularly polarized incident fields, respectively. Figures 6(d)–6(f) represent the experimentally observed transmitted SOP on the Poincaré sphere as a function of the rotation angle ϕ of the K-mirror for linearly, elliptically, and circularly polarized incident fields, respectively. The corresponding theory plots for the Dove prism and K-mirror are shown in Figs. 5(a)–5(c)

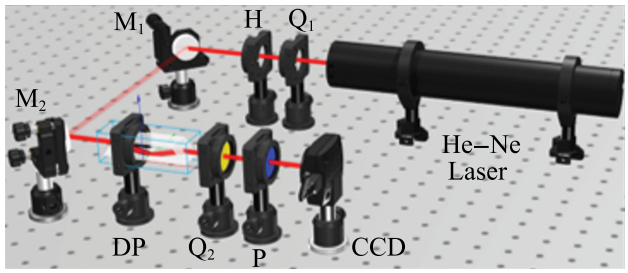

Fig. 4. Experimental setup for measuring the induced polarization changes due to a rotating Dove prism and a K-mirror. M, mirror; H, half-wave plate; Q, quarter-wave plate; DP, Dove prism; P, polarizer.

Table 1. Attributes of K-Mirrors with Different Metal Coatings to Achieve the Minimum D for Clear Aperture $h = 2.5$ cm

					% of Mean Polarization Change		
Metal	Refractive Index n_M	Base Angle β	Length L (cm)	Height H (cm)	Linear	Elliptical	Circular
Aluminum	$1.2685 + 7.2840i$	10.41°	27.22	3.84	6.71	12.85	13.12
Gold	$0.1955 + 3.2582i$	19.95°	13.78	4.13	2.16	4.20	4.31
Silver	$0.1568 + 3.8060i$	17.88°	15.50	4.04	1.52	2.96	3.04

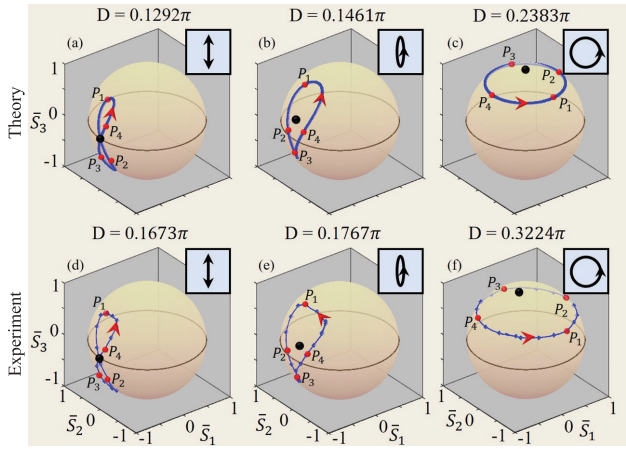

Fig. 5. Transmitted SOP as a function of the Dove prism rotation angle ϕ. (a), (b), and (c) Poincaré sphere representations of the transmitted SOP corresponding to linearly, elliptically, and circularly polarized incident fields, respectively. (d), (e), and (f) Corresponding representations of the experimentally measured transmitted SOP. The inset, as well as the black dot on the Poincaré sphere, represents the incident SOP. The sense of the rotation of the Dove prism is marked with a red arrow and points P_1 to P_4.

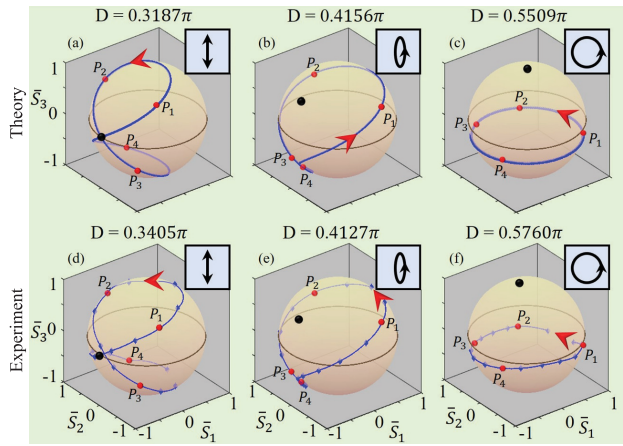

Fig. 6. Transmitted SOP as a function of the K-mirror rotation angle ϕ. (a), (b), and (c) Poincaré sphere representations of the transmitted SOP corresponding to linearly, elliptically, and circularly polarized incident fields, respectively. (d), (e), and (f) Corresponding representations of the experimentally measured transmitted SOP. The inset, as well as the black dot on the Poincaré sphere, represents the incident SOP. The sense of the rotation of the K-mirror is marked with a red arrow and points P_1 to P_4.

and Figs. 6(a)–6(c), respectively. The numerically calculated and experimentally measured D values for all the above cases are indicated in Figs. 5 and 6. We find that, although there is an excellent match between theory and experiment for the K-mirror, the match is not so good in the case of a Dove prism. This is due to the fact that it is much easier to achieve good alignment with a K-mirror than with a Dove prism. As a result, the experimentally observed values of D in the case of a Dove prism are much higher than the theory.

In conclusion, in this paper, we have theoretically and experimentally investigated the polarization changes induced by a rotating K-mirror for different incident states of polarization. For quantifying such polarization changes, we have defined a quantity that we refer to as the mean polarization change D. In our numerical studies, we have found that a K-mirror with base angle $\beta = 17.88°$ can reduce D to about 0.03π, for any incident state of polarization; however, reducing D to the same extent with a Dove prism is practically unviable. Hence, K-mirrors are more suitable than Dove prisms in applications in which the polarization changes need to be minimum. This can have important implications for applications that require wavefront rotations with minimum possible polarization changes.

Funding. Science and Engineering Research Board (Grant No. STR/2021/000035); Department of Science and Technology, Ministry of Science and Technology, India (DST/ICPS/QuST/Theme-1/2019); University Grants Commission (521572).

Acknowledgment. SK acknowledges the University Grant Commission (UGC), Government of India.

Disclosures. The authors declare no conflicts of interest.

Data availability. Data underlying the results presented in this paper are not publicly available at this time but may be obtained from the authors upon reasonable request.

Supplemental document. See Supplement 1 for supporting content.

[†]These authors contributed equally to this work.

REFERENCES

1. M. J. Padgett and J. P. Lesso, "Dove prisms and polarized light," J. Mod. Opt. **46**, 175–179 (1999).
2. I. Moreno, "Jones matrix for image-rotation prisms," Appl. Opt. **43**, 3373–3381 (2004).
3. J. Leach, J. Courtial, K. Skeldon, S. M. Barnett, S. Franke-Arnold, and M. J. Padgett, "Interferometric methods to measure orbital and spin, or the total angular momentum of a single photon," Phys. Rev. Lett. **92**, 013601 (2004).
4. Y.-D. Liu, C. Gao, and X. Qi, "Field rotation and polarization properties of the Porro prism," J. Opt. Soc. Am. A **26**, 1157–1160 (2009).
5. H. Di Lorenzo Pires, H. C. B. Florijn, and M. P. van Exter, "Measurement of the spiral spectrum of entangled two-photon states," Phys. Rev. Lett. **104**, 020505 (2010).
6. W. H. Peeters, E. J. K. Verstegen, and M. P. van Exter, "Orbital angular momentum analysis of high-dimensional entanglement," Phys. Rev. A **76**, 042302 (2007).
7. H. D. L. Pires, J. Woudenberg, and M. P. van Exter, "Measurement of the orbital angular momentum spectrum of partially coherent beams," Opt. Lett. **35**, 889–891 (2010).
8. J. Hou, M. Liang, D. Wang, and Y. Deng, "Design and analysis of a five-mirror derotator with minimal instrumental polarization in astronomical telescopes," Opt. Express **26**, 19356–19370 (2018).
9. I. Moreno, G. Paez, and M. Strojnik, "Dove prism with increased throughput for implementation in a rotational-shearing interferometer," Appl. Opt. **42**, 4514–4521 (2003).
10. S.-C. Chu, C.-S. Yang, and K. Otsuka, "Vortex array laser beam generation from a Dove prism-embedded unbalanced Mach-Zehnder interferometer," Opt. Express **16**, 19934–19949 (2008).
11. R. Mohanty, C. Joenathan, and R. Sirohi, "Speckle-shear interferometry with double dove prisms," Opt. Commun. **47**, 27–30 (1983).
12. Y. Zhi, R. Lu, B. Wang, Q. Zhang, and X. Yao, "Rapid super-resolution line-scanning microscopy through virtually structured detection," Opt. Lett. **40**, 1683–1686 (2015).
13. H. Pantsar, P. Laakso, M. Aikio, J. Huopana, H. Herfurth, and S. Heinemann, "Advanced beam steering in helical drilling," Int. Congr. Appl. Lasers Electro-Opt. **2009**, 23–29 (2009).
14. R. L. Wildey, "Spatial filtering of astronomical photographs," Publ. Astronom. Soc. Pac. **79**, 220–225 (1967).

15. H. Fujii and Y. Ohtsuka, "Rotational filtering for randomly oriented pattern recognition," Opt. Commun. **36**, 255–257 (1981).
16. O. R. Bolduc, L. S. Live, and J.-F. Masson, "High-resolution surface plasmon resonance sensors based on a Dove prism," Talanta **77**, 1680–1687 (2009).
17. P. Z. Takacs, E. L. Church, C. J. Bresloff, and L. Assoufid, "Improvements in the accuracy and the repeatability of long trace profiler measurements," Appl. Opt. **38**, 5468–5479 (1999).
18. D. J. Armstrong and A. V. Smith, "Demonstration of improved beam quality in an image-rotating optical parametric oscillator," Opt. Lett. **27**, 40–42 (2002).
19. M. A. Alonso and A. N. Jordan, "Can a Dove prism change the past of a single photon?" Quantum Stud.: Math. Foundat. **2**, 255–261 (2015).
20. J. Leach, M. J. Padgett, S. M. Barnett, S. Franke-Arnold, and J. Courtial, "Measuring the orbital angular momentum of a single photon," Phys. Rev. Lett. **88**, 257901 (2002).
21. F.-X. Wang, W. Chen, Y.-P. Li, G.-W. Zhang, Z.-Q. Yin, S. Wang, G.-C. Guo, and Z.-F. Han, "Single-path sagnac interferometer with Dove prism for orbital-angular-momentum photon manipulation," Opt. Express **25**, 24946–24959 (2017).
22. N. González, G. Molina-Terriza, and J. P. Torres, "How a Dove prism transforms the orbital angular momentum of a light beam," Opt. Express **14**, 9093–9102 (2006).
23. I. Moreno, G. Paez, and M. Strojnik, "Polarization transforming properties of Dove prisms," Opt. Commun. **220**, 257–268 (2003).
24. D. H. Goldstein, *Polarized Light* (CRC Press, 2011).
25. H. Z. Sar-El, "Revised Dove prism formulas," Appl. Opt. **30**, 375–376 (1991).